Diffusive nitrous oxide (N_2O) fluxes across the sediment-water-atmosphere interfaces in aquaculture shrimp ponds in a subtropical estuary: Implications for climate warming

Yalan Tian[a,b], Ping Yang[a,b*], Hong Yang[c,d], Huimin Wang[e], Linhai Zhang[a,b], Chuan Tong[a,b], Derrick Y.F. Lai[f], Yongxin Lin[a,b], Lishan Tan[g], Yan Hong[a,b], Chen Tang[a,b], Kam W. Tang[h*]

[a]*School of Geographical Sciences, Fujian Normal University, Fuzhou 350007, P.R. China*

[b]*Key Laboratory of Humid Subtropical Eco-geographical Process of Ministry of Education, Fujian Normal University, Fuzhou 350007, P.R. China*

[c]*College of Environmental Science and Engineering, Fujian Normal University, Fuzhou 350007, P.R. China*

[d]*Department of Geography and Environmental Science, University of Reading, Reading, RG6 6AB, UK*

[e]*Fujian Provincial Geomatics center, Fuzhou 350007, P.R. China*

[f]*Department of Geography and Resource Management, The Chinese University of Hong Kong, Hong Kong, China*

[g]*State Key Laboratory of Estuarine and Coastal Research, East China Normal University, Shanghai, China*

[h]*Department of Biosciences, Swansea University, Swansea SA2 8PP, U. K.*

***Correspondence to:**

Ping Yang (yangping528@sina.cn); Kam W. Tang (k.w.tang@swansea.ac.uk)

Telephone: 086-0591-87445659 **Fax:** 086-0591-83465397

ABSTRACT

Emissions of the potent greenhouse gas nitrous oxide (N_2O) from aquaculture remain a large knowledge gap in the global N_2O budget. The water column and the sediment of aquaculture ponds present very different environmental conditions, but their relative contributions to N_2O production and emission are poorly resolved. We sampled three aquaculture ponds in the Min River Estuary in southeastern China monthly throughout the farming season. Based on the dissolved N_2O concentrations within the water column and in sediment porewater, we calculated the diffusive N_2O fluxes across the water-atmosphere interface (WAI) and sediment-water interface (SWI). The diffusive N_2O flux averaged 216.9 nmol m^{-2} h^{-1} across WAI and 16.0 nmol m^{-2} h^{-1} across SWI. The estimated N_2O production rate under steady-state condition was 0.13 nmol L^{-1} h^{-1} in the water column and 1.07 nmol L^{-1} h^{-1} in sediment porewater. Hence, the water column compartment and the sediment compartment of the aquaculture ponds played different roles in N_2O dynamics. Based on our data, it is calculated that China's coastal aquacultural ponds would emit 0.2 Gg N_2O yr^{-1}, or less than 1% of all aquaculture N_2O emission in China. Therefore, coastal shrimp aquaculture has a relative minor climate impact compared to other aquaculture operations. Future studies should examine the role of N-cycling functional genes on N_2O production and the mechanisms regulating N_2O emission from aquaculture ecosystems.

Keywords: Nitrous oxide (N_2O) fluxes; Sediment-water interface (SWI); Water-atmosphere interface (WAI); Nitrogen substrate; Temperature; Aquaculture ponds

1. Introduction

Nitrous oxide (N_2O) is an ozone-depleting greenhouse gas (GHG), contributing substantially to radiative forcing and global climate change (Maavara et al., 2018; Quick et al., 2019; Ravishankara et al., 2009). The Industrial Revolution and intensive fertilization for farming have increased nitrogen availability significantly in both land and water environments (Swaney et al., 2012; Howarth et al., 1996; Zhang et al., 2020), which in turn has caused the increase in atmospheric N_2O. N_2O has increased to 335.3 ppbv this year (NOAA, 2022), exceeding the preindustrial concentration by ~24%, and the agricultural sector contributes ~60% (4.3 Tg N yr^{-1}) of the global N_2O emissions from anthropogenic activities (Tian et al., 2020; Webb et al., 2021). China has promised to be carbon neutral by 2060 (Yang et al., 2022). To effectively mitigate the impact of climate change, it is therefore crucial to better understand the N_2O biogeochemical processes in various agriculture ecosystems.

Nitrous oxide can be produced in soil (or sediment) and water by two main microbial processes, nitrification and denitrification (Audet et al., 2017; Li et al., 2021; Wrage et al., 2005; Wu et al., 2021), with oxygen (O_2) and nitrogen (N) availabilities being important controlling factors (Murray et al., 2015; Xiao et al., 2019a; Yang et al., 2020a). Similar to crop fields, aquaculture systems (e.g., aquaculture ponds) receive heavy N loadings and are hotspots for N_2O production (Hu et al., 2012; Yang et al., 2020a; Yuan et al., 2019, 2021) and emission (Paudel et al., 2015; Ye et al., 2022; Yogev et al., 2018). An aquaculture system contains two compartments—the water column and the sediment, both of which can contribute to N_2O production but are characterized by different reduction-oxidation conditions and microbial community compositions (Beaulieu et al., 2015; Freing et al., 2012; Yuan et al., 2021). The anoxic sediment receives a large amount of organic matter (OM) from animal feces and residual feeds (Chen et al., 2016; Yang et al., 2021), where microbial mineralization of the OM fuels N_2O production (Lin and Lin, 2022; Yuan et al., 2021). On the other hand, the overlying water column tends to be better aerated and may support aerobic microbial activities, such as nitrification.

Although efforts have been made to quantify N_2O emissions from aquaculture systems, there is a paucity of information on the relative contributions of the two compartments (Hu et al., 2012). To close the knowledge gap, we analysed the diffusive N_2O fluxes across the SWI and the WAI of aquaculture ponds in southeastern China. The objectives were to: (1) characterize the temporal variations in diffusive N_2O fluxes across the sediment-water-atmosphere interfaces; (2) explore the environmental factors that drive the temporal variations in N_2O fluxes; (3) compare the roles of sediment and water in N_2O production and emission from the aquaculture ponds. We hypothesized that: (1) N_2O fluxes would exhibit distinct temporal variations in response to differences in environmental variables (e.g., temperature and nitrogen availability); (2) the water column would contribute more than the sediment to the overall N_2O emission to air.

2. Materials and methods

2.1. Study area

Our research area is located in the Shanyutan wetland of the Min River Estuary

(MRE), southeastern China (Figure 1). The region has a humid subtropical monsoon climate (Tong et al., 2010), with a mean annual temperature of 19.6 °C and an average annual precipitation of 1,390 mm (Yang et al., 2020b). The wetland has three dominant vegetation types: two with the native species *Cyperus malaccensis* and *Phragmites australis,* and one with the invasive species *Spartina alterniflora*. During the past decades, large extent of the MRE tidal saltmarshes (mainly dominated by *C. malaccensis* and *S. alterniflora*) were converted to aquaculture ponds for shrimp (*Litopenaeus vannamei*) due to rising demand for seafood (Strokal et al., 2021; Yang et al., 2020c). Shrimp farming typically begins in May and ends in November, with one crop of shrimp produced annually. For more details of the aquaculture operation, please see Yang et al. (2020c). In this study, three aquaculture ponds of ~1.5 m deep were selected for monthly sampling of water and sediment from April 2019 to January 2020, for a total of 10 sampling campaigns in each pond. In each pond, samples were collected from three sites: one near the bank, one in the feeding zone, and one at the center of the pond.

2.2. Sediment collection and bulk properties

Three surface sediments (top 15 cm) were collected at each site using a steel cylinder (5 cm in diameter), stored in sterile sample bags and transported in a cooler to the laboratory within 4–6 hr. All samples were stored at 4 ºC, and analyzed within 72 hr. In the laboratory, the samples were analyzed for physicochemical properties of sediments, dissolved N_2O concentrations and physicochemical properties of porewater, as explained below.

Subsamples of sediment were freeze-dried, homogenized and ground to fine powder to determine pH and salinity. Sediment pH was determined via a pH meter (Thermo Fisher Scientific, Sunnyvale, California, USA) in a sediment-to-water ratio of 1:2.5 (w/v with added deionized water). Sediment salinity (SAL) was measured by a Eutech Instruments-Salt6 salinity meter (Thermo Fisher Scientific, San Francisco, California, USA) in a sediment-to-water ratio 1:5 (w/v). Soil water content (SWC) and bulk density (BD) were determined after drying fresh soil at 105 °C for 48 h (Percival and Lindsay, 1997; Yin et al., 2019); weight loss after drying was used to calculate sediment porosity (POR) (Zhang et al., 2013). *In situ* sediment temperature (T_S) were measured by a portable temperature meter (IQ150, IQ Scientific Instruments, Carlsbad, California, USA).

2.3. N_2O concentration and dissolved chemicals in sediment porewater

The dissolved N_2O concentrations in sediment porewater was measured according to Dutta et al. (2015). Briefly, a subsample of sediment (6 cm^3) was collected via a 10 mL syringe, transferred to a 55-mL glass serum vial, and then sealed using an open-topped screw cap and a halobutyl rubber septum. The vial was shaken vigorously in an oscillator (IS-RDD3, China) for 10 min to achieve gas equilibrium between the slurry and the headspace. The concentration of headspace N_2O (approximately 10 mL) was then analysed on a gas chromatograph (GC) with an electron capture detector (ECD) (Shimadzu GC-2014, Kyoto, Japan). Three N_2O gas standards, namely 0.3, 0.4, and 1.0 ppm, were used in the calibration. The detection limit for N_2O was 0.02 ppm, and the relative standard deviations of N_2O were ±4.5% in 24 h. The calculation of sediment porewater dissolved N_2O concentration (nmol L^{-1}) followed the method of Ding et al. (2005) and Johnson et al. (1990).

The rest of the bulk sediment was centrifugated at 5000 rpm for 10 min (Cence® L550, De Vittor et al., 2012) to extract porewater. After being filtered through 0.45 μm acetate fiber membranes (Biotrans™ nylon membranes), the porewater filtrates were analyzed for the levels of nitrate-nitrogen (NO_3^--N) and ammonia-nitrogen (NH_4^+-N) on a flow injection analyzer (Skalar Analytical SAN^{++}, Netherlands), and Cl^- and SO_4^{2-} on an ion chromatograph (Dionex 2100, Thermo Fisher Scientific, Sunnyvale, California, USA).

2.4. Water sample collection and analysis

Water column samples were taken from the surface layer (~10 cm below the surface) and the bottom layer (~5 cm above the sediment) using a 1.5-L organic glass hydrophores, and then transferred into 150 mL polyethylene bottles and 55 mL pre-weighed serum glass bottles. All water samples were preserved with saturated $HgCl_2$ solution (~0.5 mL) (Borges et al., 2018; Marescaux et al., 2018) and transported in a cooler to the laboratory within 4–6 hr. Approximately 100 mL water sample was filtered through a 0.45 μm acetate fiber membrane (Biotrans™ nylon membranes) and the filtrate was used to analyze the levels of NO_3^--N and NH_4^+-N, total dissolved nitrogen (TDN), Cl^- and SO_4^{2-}.

Dissolved N_2O concentrations were determined by headspace equilibration and gas chromography (Yu et al., 2013; Musenze et al., 2014). Briefly, nitrogen gas (N_2; >99.9%

purity) was injected into each serum glass bottle to displace a 25-mL headspace and the bottle was shaken vigorously for 10 min (IS-RDD3, China) to attain air-water equilibrium. After waiting for 0.5 hour, a 5 mL headspace sample was extracted and injected into a gas chromatograph as explained earlier (see Section 2.3). The *in situ* dissolved N_2O concentrations (nmol L^{-1}) were calculated according to Yu et al. (2013) and Musenze et al. (2014).

2.5. Diffusive N_2O fluxes across the sediment-water interface (SWI)

The diffusive N_2O fluxes across SWI ($F_{S\text{-}W}$, nmol m^{-2} h^{-1}; positive values indicate N_2O fluxes from sediment to water) were calculated as (Gruca-Rokosz and Tomaszek, 2015; Tan et al., 2014):

$$F_{S-W} = D_S \times \Delta C/\Delta Z = (D_w \times \text{POR}) \times (C_S - C_W)/\Delta Z \qquad \text{(Eq. 1)}$$

where D_S is the diffusion coefficient of N_2O in sediment (cm^2 s^{-1}); $\Delta C/\Delta Z$ is the gradient for dissolved N_2O concentration with depth; POR is sediment porosity; C_S is dissolved N_2O concentration in sediment porewater (nmol L^{-1}); C_W is the dissolved N_2O concentration in overlying water (near the sediment surface) (nmol L^{-1}); Z is diffusion distance (cm); D_w is the diffusion coefficient of N_2O in water (cm^2 s^{-1}), which was calculated as:

$$D_W = -6.0 \times 10^{-9} T_W^2 + 10^{-9} T_W - 3.0 \times 10^{-7} \qquad \text{(Eq. 2)}$$

where T_W is the temperature in overlying water (near the sediment surface) (°C).

2.6. Diffusive N_2O fluxes across the water-atmosphere interface (WAI)

The diffusive N_2O fluxes across SWI ($F_{W\text{-}A}$, nmol m^{-2} h^{-1}; positive values indicate

N_2O fluxes from water to air) were calculated as (Musenze et al., 2014):

$$F_{\mathrm{W-A}} = [2.07 + (0.215 \times U_{10}^{1.7})](Sc/660)^{-n} \times (C_{\mathrm{W}} - C_{\mathrm{eq}}) \qquad \text{(Eq. 3)}$$

where C_W is the dissolved N_2O level (nmol L^{-1}) in the surface water; C_{eq} is the N_2O level in water that is in equilibrium with air at the *in situ* temperature; U_{10} is the frictionless wind speed (W_S; m s^{-1}) at 10 m height above the water surface according to Crusius and Wanninkhof (2003); *Sc* is the Schmidt number for N_2O (Wanninkhof, 1992); *n* is a constant that varies between 0.50 (W_S>3 m s^{-1}) and 0.66 (for W_S≤3 m s^{-1}) (Cole and Caraco, 1998).

2.7. Auxiliary data

Meteorological parameters, including air pressure (A_P), wind speed (W_S) and air temperature (T_A), were collected by an automated meteorological station on site. In each sampling campaign, *in situ* water salinity (Sal), temperature (T_W) and dissolved oxygen (DO) were measured by a Eutech Instruments-Salt6 salinity meter (Thermo Fisher Scientific, San Francisco, California, USA), a temperature meter (IQ150, IQ Scientific Instruments, Carlsbad, California, USA) and a multiparameter probe (550A YSI, USA), respectively.

2.8. Statistical analysis

All data were checked for normality and homogeneity of variance before further statistical analysis. One–way ANOVA was conducted in SPSS 22.0 (IBM, Armonk, NY, USA) to explore the effects of sampling time on various environmental variables, N_2O concentrations and diffusive N_2O fluxes. Spearman correlation analysis was performed to examine the relationships between diffusive N_2O fluxes (or dissolved N_2O concentrations) and environmental parameters, using R corrplot and Hmisc packages. The extent to which environmental variables regulated the temporal variations in diffusive N_2O fluxes (or dissolved N_2O concentrations) was analysed using Redundancy Analysis (RDA) in CANOCO 5.0 (Microcomputer Power, Ithaca, USA). The significance level was set at $p<0.05$ for all analyses.

3. Results

3.1. Physical and chemical characteristics

The physicochemical properties of porewater and surface water are shown in Figure 2. Air, water and sediment temperatures increased from April toward July and August, then decreased toward January. Across all sampling months, the mean temperature, NO_3^--N and NH_4^+-N concentrations in sediment porewater were 20.25±0.59 ºC, 0.22±0.03 mg L^{-1} and 0.33±0.04 mg L^{-1}, respectively, which were significantly lower than in the surface water (25.36±1.01 ºC, 1.19±0.20 mg L^{-1} and 0.52±0.13 mg L^{-1}, resepctively) ($p<0.05$ or <0.01).

3.2. Dissolved N_2O concentration in sediment porewater and water column

Dissolved N_2O concentration varied significantly over time ($p<0.01$; Figure 3). It ranged from 2.11±0.18 to 21.68±2.60 nmol L^{-1} in the surface water, 1.83±0.11 to 22.04±5.54 nmol L^{-1} in the bottom water, and 5.02±0.63 to 40.48±5.31 nmol L^{-1} in the sediment porewater (Figure 3). The mean N_2O concentration was significantly higher in sediment porewater (18.94±3.05 nmol L^{-1}), followed by bottom water (9.88±2.11 nmol

L^{-1}) and surface water (9.29±2.12 nmol L^{-1}) (p<0.001). The highest N_2O concentration was observed in September in the sediment porewater and in July in the surface water and bottom water (Figure 3).

3.3. N_2O fluxes across the sediment–water-atmosphere interfaces

The diffusive N_2O fluxes across the SWI were always positive (ranged 1.51–48.84 nmol m^{-2} h^{-1}; Figure 4a), indicating net N_2O releases from the sediment to the overlying water. The N_2O fluxes across the SWI varied significantly between months ($F_{df=9}$=4.962, p=0.001) with considerably higher values from August to October (Figure 4a).

The diffusive N_2O fluxes across the WAI of the ponds showed significant temporal variations ($F_{df=9}$=32.227, p<0.001; Figure 4b), with higher fluxes from June to August, and lower fluxes from November to January (Figure 4b). Overall, the diffusive N_2O fluxes across WAI ranged from 25.06 to 507.87 nmol m^{-2} h^{-1} (Figure 4b), indicating that the aquaculture ponds were an N_2O emission source to the atmosphere.

Across all the sampling campaigns, the mean diffusive N_2O flux across WAI (216.85 ± 55.52 nmol m^{-2} h^{-1}) was an order of magnitude higher than that across SWI (16.00 ± 4.60 nmol m^{-2} h^{-1}) ($F_{df=1}$ = 38.319 p < 0.01).

3.4. Environmental drivers of N_2O concentrations and fluxes

Spearman correlation analysis showed that N_2O fluxes across SWI (or porewater N_2O concentrations) correlated positively with T_S (p<0.001) and NO_3^--N (p<0.01), but negatively with sediment salinity (p<0.01), porewater Cl^- (p<0.05) and SO_4^{2-} concentrations (p<0.01) (Figure 5a). N_2O fluxes across WAI (or water column N_2O

concentrations) correlated positively with T_A, T_W, NO_3^--N and TDN (p<0.01 or p<0.001), but negatively with A_P, DO, pH, salinity, Cl^- and SO_4^{2-} concentrations (p<0.01 or p<0.001) (Figure 5b).

Based on the results of RDA, T_S (explaining 57.2% of the variations) and NO_3^--N (16.9%) were the variables that explained most of the temporal variations in N_2O fluxes across SWI (or porewater N_2O concentrations) (Figure 6a), whereas variations in N_2O fluxes across WAI (or water column N_2O concentrations) were mostly explained by T_W, (64.6%), followed by NO_3^--N (21.4%) and TDN (8.8%) (Figure 6b).

4. Discussion

Nitrous oxide emissions from agriculture have been a main focus in climate science due to the increase in agricultural land use and application of fertilizer (Del Grosso et al., 2008; Shcherbak et al., 2014). While the estimates of agricultural N_2O emissions are reasonably well constrained at the global level, uncertainties persist at the regional and local levels (Reay et al., 2012). Earlier studies also highlighted that N_2O emissions from aquaculture systems remain a critical knowledge gap, especially considering the rapid expansion of the aquaculture sector worldwide (Reay et al., 2012).

The whiteleg shrimp *Litopenaeus vannamei* is one of the main species farmed in small-hold earthen ponds along the China's coast (BFMA, 2019). The sediment and the water column of aquaculture ponds present very different reduction-oxidation environments to drive the different N_2O production pathways, for example, via incomplete denitrification in anoxic condition and nitrification in oxic condition, using

NO_3^--N or NH_4^+-N as substrate (Hu et al., 2012, 2013; Yuan et al., 2021; Yang et al., 2020d). In contrast to the expectation that the sediment is a sink of nitrogenous substrates from deposition of animal wastes and excess feed (Avnimelech and Ritvo, 2003; Hargreaves et al., 1998), our data showed that both NO_3^--N and NH_4^+-N concentrations were higher in the water column than in the sediment porewater (Figure 2). This perhaps reflects the high efficiency of the shrimp to convert feed to biomass and its ability to recycle nutrients within the water column (Avnimelech and Ritvo, 2003; Lacoste and Gaertner-Mazouni, 2016; Zhang et al., 2016). The large increase in surface-water NO_3^--N concentration in July–October was likely caused by the increased use of feed and increased feeding activity of the shrimp during its summer growth burst.

Despite the much lower NO_3^--N concentration in the sediment porewater than the water column (Figure 2), sediment porewater N_2O concentration was comparable to or more than twice that in the overlying water (Figure 3). These observations suggest that N_2O was produced mainly via denitrification and accumulated in the anoxic sediment (Blackburn and Blackburn, 1992), whereas N_2O production via denitrification (using NO_3^--N) or nitrification (using NH_4^+-N) was rather limited in the water column.

Movement of the shrimp in the pond bottom could disturb the sediment and accelerate chemical exchanges between the sediment and the overlying water. Previous experimental studies have suggested that bioturbation by *L. vannamei* released nutrients from the sediment and increased oxygen consumption in the overlying water (Yang et al., 2017; Zhang et al., 2015); however, those measurements were made in artificial enclosures where the shrimp may not behave normally. In this study, we observed that sediment porewater N_2O concentration was consistently higher than that in the bottom water (~5 cm above sediment) on all but two occasions (Figure 3); therefore, there was no evidence of bioturbation by the shrimp in the pond that would have destroyed the N_2O gradient across the water-sediment interface.

Based on the N_2O distributions, we calculated the N_2O fluxes across the SWI and the WAI (Figure 4). The N_2O fluxes across SWI were highest in the summer months (August-October), coinciding the higher porewater NO_3^--N concentrations and sediment temperatures (Figure 2a and 2b), both of which would have increased microbial denitrification activity in the sediment (Hu et al., 2012; Murray et al., 2015; Reisinger et al., 2016). The N_2O fluxes across WAI increased earlier, reaching a maximum in July, which was also consistent with the earlier rise in water temperature and water column NO_3^--N concentration (Figure 2). These explanations were further supported by Spearman correlation and RDA analyses (Figures 5 and 6).

Averaging across the study period, N_2O flux across WAI was an order of magnitude higher than N_2O flux across SWI, implying that the water column played a larger role in emitting N_2O from the aquaculture pond. Overall, the N_2O emissive fluxes from the shrimp ponds were comparable to other aquaculture ponds, static waters (reservoirs and lakes) and running waters (rivers and estuaries), but considerably less than the highly eutrophic waters (Table 1). Coastal shrimp aquaculture in China is dominated by small-hold earthen ponds that cover a total area of ~2400 km^2 (BFMA, 2019), the majority of which are poorly monitored for their greenhouse gas emissions. Using data from this study, we estimate that coastal shrimp ponds in China would emit 0.2 Gg N_2O yr^{-1} or 4.5×10^{-3} Gg N yr^{-1}. A recent study estimated that N_2O emission from marine and freshwater aquacultures in China amounts to ~16.7 Gg N y^{-1} (Zhou et al., 2021). Notwithstanding the uncertainties associated with the feed conversion rates and emission factors used in Zhou et al.'s study, our calculations suggest that coastal shrimp ponds contribute <1 % of the aquaculture N_2O emission in China.

Assuming the aquaculture pond ecosystem was in steady state, we may estimate the N_2O production rates in the sediment and the water column compartments as follows: We considered a sediment surface area of 1 m^2. Assuming that deposition of nitrogenous substrates for N_2O production was limited to the top 15 cm sediment and given the average N_2O flux of 16 nmol m^{-2} h^{-1} across SWI and an average sediment porewater N_2O concentration of 18.94 nmol L^{-1}, the N_2O turnover time for a 1 m^2 × 15 cm sediment compartment would be 17.75 hours and the equivalent N_2O net production rate would be 1.07 nmol L^{-1} h^{-1} under a steady-state condition. For a water column of 1 m^2 surface area × 1.5 m depth (average depth of the aquaculture pond), the N_2O concentrations were similar between surface water (9.29 nmol L^{-1}) and bottom water (9.88 nmol L^{-1}); therefore, we used the average concentration of 9.59 nmol L^{-1}. The net loss of N_2O from the water column compartment through emission to air would be the difference between the average WAI flux (216.85 nmol m^{-2} h^{-1}) and SWI flux (16.00 nmol m^{-2} h^{-1}), i.e., 200.85 nmol m^{-2} h^{-1}. The water-column N_2O turnover time would be 9.59 × 1500 ÷

200.85 = 71.58 hours, and the equivalent net N_2O production rate in the water column would be 0.13 nmol L^{-1} h^{-1}. There is a lack of empirical data on ambient N_2O production rates in aquaculture ponds; nevertheless, our estimates fall within the range observed in eutrophic coastal waters (De Wilde and De Bie, 2000; Punshon and Moore, 2004).

5. Conclusions

Overall, our results show that the sediment compartment and the water column compartment played opposite roles in N_2O dynamics within the aquaculture ponds: The sediment had a much higher N_2O production rate than the water column, whereas the water column contributed a much higher overall emission to air. Environmental temperatures and nitrogenous substrates were the main controlling factors in both compartments. Although our data showed that coastal aquaculture shrimp ponds were a net source of N_2O emission to the atmosphere, their overall contributions were relative minor compared to other aquaculture operations in China; therefore, shrimp aquaculture remains a preferred solution to the growing demand for animal proteins without exacerbating the climate impact.

Acknowledgements

This research was supported jointly by the National Natural Science Foundation of China (41801070, 41671088), the National Natural Science Foundation of Fujian Province (2022R1002006; 2020J01136), and the Minjiang Scholar Programme.

References

Audet, J., Wallin, M.B., Kyllmar, K., Andersson, S., Bishop, K., 2017. Nitrous oxide emissions from streams in a Swedish agricultural catchment. Agr. Ecosyst. Environ. 236, 295–303. http://dx.doi.org/10.1016/j.agee.2016.12.012

Avnimelech, Y., Ritvo, G., 2003. Shrimp and fish pond soils: processes and management. Aquaculture 220, 549–567. https://doi.org/10.1016/S0044-8486(02)00641-5.

Blackburn, T.H., Blackburn, N.D., 1992. Model of nitrification and denitrification in marine sediments. FEMS Microbiol. Lett. 100(1–3), 517–521. https://doi.org/10.1016/0378-1097(92)90255-M

Baranov, V., Lewandowski, J., Krause, S., 2016. Bioturbation enhances the aerobic respiration of lake sediments in warming lakes. Biol. Lett. 12, 20160448. http://dx.doi.org/10.1098/rsbl.2016.0448

Barnes, J., Upstill-Goddard, R.C., 2011. N_2O seasonal distributions and air-sea exchange in UK estuaries: Implications for the tropospheric N_2O source from European coastal waters. J. Geophys. Res. 116, G01006. https://doi.org/10.1029/2009JG001156

Beaulieu, J.J., Nietch, C.T., Young, J.L., 2015. Controls on nitrous oxide production and consumption in reservoirs of the Ohio River Basin. J. Geophys. Res.-Biogeo. 120(10), 1995–2010. https://doi.org/10.1002/2015jg002941

Beaulieu, J.J., Shuster, W.D., Rebholz, J.A., 2010. Nitrous oxide emissions from a large, impounded river: The Ohio River. Environ. Sci. Technol. 44, 7527–7533. https://doi.org/10.1021/es1016735

BFMA (Bureau of Fisheries of the Ministry of Agriculture), 2019. China Fishery Statistics Yearbook. China Agriculture Press, Beijing (in Chinese).

Borges, A. V., Darchambeau, F., Lambert, T., Bouillon, S., Morana, C., Brouyère, S., Hakoun, V., Jurado, A., Tseng, H.-C., Descy, J.-P., Roland, F.A.E., 2018. Effects of agricultural land use on fluvial carbon dioxide, methane and nitrous oxide concentrations in a large European river, the Meuse (Belgium). Science of the Total Environment, 610-611, 342–355. https://doi.org/10.1016/j.scitotenv.2017.08.047

Burgos, M., Ortega, T., Forja, J.M., 2017. Temporal and spatial variation of N_2O production from estuarine and marine shallow systems of Cadiz Bay (SW, Spain). Sci. total Environ. 607–608, 141–151.

https://doi.org/10.1016/j.scitotenv.2017.07.021
Butterbach-Bahl, K., Baggs, E.M., Dannenmann, M., Kiese, R., Zechmeister-Boltenstern, S., 2013. Nitrous oxide emissions from soils: how well do we understand the processes and their controls? Phil. Trans. R. Soc. B 368, 20130122. https://doi.org/10.1098/rstb.2013.0122
Chen, Y., Dong, S.L., Wang, F., Gao, Q.F., Tian, X.L., 2016. Carbon dioxide and methane fluxes from feeding and no-feeding mariculture ponds. Environ. Pollut. 212, 489–497. https://doi.org/10.1016/j.envpol.2016.02.039
Cole, J.J., Caraco, N.F., 1998. Atmospheric exchange of carbon dioxide in a low-wind oligotrophic lake measured by the addition of SF_6. Limnol. Oceanogr. 43, 647–656. https://doi.org/10.4319/lo.1998.43.4.0647
Cooper, R.J., Wexler, S.K., Adams, C.A., Hiscock, K.M., 2017. Hydrogeological controls on regional-scale indirect nitrous oxide emission factors for rivers. Environ. Sci. Technol. 51, 10440–10448. https://doi.org/10.1021/acs.est.7b02135
Crusius, J., Wanninkhof, R., 2003. Gas transfer velocities measured at low wind speed over a lake. Limnol. Oceanogr. 48(3), 1010–1017.
Dalsgaard, T., Stewart, F. J., Thamdrup, B., Brabandere, L. D., Revsbech, N. P., Ulloa, O., Canfield, D.E.,DeLong, E.F., 2014. Oxygen at nanomolar levels reversibly suppresses process rates and gene expression in anammox and denitrification in the oxygen minimum zone off northern Chile. mBio, 5(6), e01966-14. https://doi.org/10.1128/mBio.01966-14
De Vittor, C., Faganeli, J., Emili, A., Covelli, S., Predonzani, S., Acquavita, A., 2012. Benthic fluxes of oxygen, carbon and nutrients in the marano and grado lagoon (northern adriatic sea, Italy). Estuar. Coast Shelf Sci. 113, 57–70. https://doi.org/10.1016/j.ecss.2012.03.031
Del Grosso, S.J., Wirth, T., Ogle, S. M., Parton, W.J., 2008. Estimating agricultural nitrous oxide emissions. EOS, Transactions American Geophysical Union, 89(51), 529-529. https://doi.org/10.1029/2008eo510001
De Wilde, H.P., De Bie, M.J., 2000. Nitrous oxide in the Schelde estuary: production by nitrification and emission to the atmosphere. Mar. Chem. 69(3-4), 203–216.

https://doi.org/10.1016/s0304-4203(99)00106-1
Descloux, S., Chanudet, V., Serça, D., Guérin, F., 2017. Methane and nitrous oxide annual emissions from an old eutrophic temperate reservoir. Sci. Total Environ. 598, 959–972. https://doi.org/10.1016/j.scitotenv.2017.04.066
Ding, W.X., Zhang, Y.H., Cai, Z.C., 2010. Impact of permanent inundation on methane emissions from a *Spartina alterniflora* coastal salt marsh. Atmos. Environ. 44, 3894–3900. https://doi.org/10.1016/j.atmosenv.2010.07.025
Dutta, M.K., Mukherjee, R., Jana, T.K., Mukhopadhyay, S.K., 2015. Biogeochemical dynamics of exogenous methane in an estuary associated to a mangrove biosphere; The Sundarbans, NE coast of India. Mar. Chem. 170, 1–10. https://doi.org/10.1016/j.marchem.2014.12.006
Fang, X.T., Zhao, J.T., Wu, S., Yu, K., Huang, J., Ding, Y., Hu, T., Xiao, S.Q., Liu, S.W., Zou, J.W., 2022. A two-year measurement of methane and nitrous oxide emissions from freshwater aquaculture ponds: Affected by aquaculture species, stocking and water management. Sci. Total Environ. 813, 151863. https://doi.org/10.1016/j.scitotenv.2021.151863
Freing, A., Wallace, D.W.R., Bange, H.W., 2012. Global oceanic production of nitrous oxide. Phil. Trans. R. Soc. B 367 (1593), 1245–1255. https://doi.org/10.1016/10.1098/rstb.2011.0360
Gonçalves, C., Brogueira, M.J., Nogueira, M., 2015. Tidal and spatial variability of nitrous oxide (N_2O) in Sado estuary (Portugal). Estuar. Coast. Shelf S. 167, 466–474. https://doi.org/10.1016/j.ecss.2015.10.028
Gruca-Rokosz, R., Tomaszek, J.A., 2015. Methane and carbon dioxide in the sediment of a eutrophic reservoir: production pathways and diffusion fluxes at the sediment–water interface. Water Air Soil Pollut. 226, 16. https://doi.org/10.1007/s11270-014-2268-3
Guérin, F., Abril, G., Tremblay, A., Delmas, R., 2008. Nitrous oxide emissions from tropical hydroelectric reservoirs. Geophys. Res. Lett. 35(6), L06404. https://doi.org/10.1029/2007GL033057
Hama-Aziz, Z.Q., Hiscock, K.M., Cooper, R.J., 2017. Indirect nitrous oxide emission

factors for agricultural field drains and headwater streams. Environ. Sci. Technol. 51, 301–307. https://doi.org/10.1021/acs.est.6b05094

Hargreaves, J.A., 1998. Nitrogen biogeochemistry of aquaculture ponds. Aquaculture, 166(3-4), 181-212. https://doi.org/10.1016/s0044-8486(98)00298-1

He, Y.X., Wang, X.F., Chen, H., Yuan, X.Z., Wu, N., Zhang, Y.W., Yue, J.S., Zhang, Q.Y., Diao, Y.B., Zhou, L.L., 2017. Effect of watershed urbanization on N_2O emissions from the Chongqing metropolitan river network, China. Atmos. Environ. 171, 70–81. https://doi.org/10.1016/j.atmosenv.2017.09.043

Herrman, K.S., Bouchard, V., Moore, R.H., 2008. Factors affecting denitrification in agricultural headwater streams in Northeast Ohio, USA. Hydrobiologia 598, 305–314. https://doi.org/10.1007/s10750-007-9164-4

Hinshaw, S.E., Dahlgren, R.A., 2013. Dissolved nitrous oxide concentrations and fluxes from the eutrophic San Joaquin River, California. Environ. Sci. Technol. 47, 1313–1322. https://doi.org/10.1021/es301373h

Hirota, M., Senga, Y., Seike, Y., Nohara, S., Kunii, H., 2007a. Fluxes of carbon dioxide, methane and nitrous oxide in two contrastive fringing zones of coastal lagoon, lake Nakaumi, Japan. Chemosphere 68, 597–603. https://doi.org/10.1016/j.chemosphere.2007.01.002

Howarth, R.W., Billen, G., Swaney, D., Townsend, A., Jaworski, N., Lajtha, K., Downing, J.A., Elmgren, R., Caraco, N., Jordan, T., Berendse, F., Freney, J., Kudeyarov, V., Murdoch, P., Zhu, Z.L., 1996. Regional nitrogen budgets and riverine N&P fluxes for the drainages to the North Atlantic Ocean: natural and human influences. Biogeochemistry 35, 75–139.

Hu, B.B., Xu, X.F., Zhang, J.F., Wang, T.L., Meng, W.Q., Wang, D.Q., 2020. Diurnal variations of greenhouse gases emissions from reclamation mariculture ponds. Estuar. Coast. Shelf. S. 237, 106677. https://doi.org/10.1016/j.ecss.2020.106677

Hu, Z., Lee, J.W., Chandran, K., Kim, S., Khanal, S.K., 2012. Nitrous oxide (N_2O) emission from aquaculture: a review. Environ. Sci. Technol. 46, 6470–6480. https://doi.org/10.1021/es300110x

Hu, Z., Lee, J.W., Chandran, K., Kim, S., Sharma, K., Brotto, A.C., Khanal, S.K., 2013. Nitrogen transformations in intensive aquaculture system and its implication to climate change through nitrous oxide emission. Bioresour. Technol. 130, 314–320. 10.1016/j.biortech.2012.12.033

Huertas1, I.E., Flecha, S., Navarro, G., Perez, F.F., de la Paz, M., 2018. Spatio-temporal variability and controls on methane and nitrous oxide in the Guadalquivir Estuary, Southwestern Europe. Aquat. Sci. 80, 29. https://doi.org/10.1007/s00027-018-0580-5

Huttunen, J.T., Vaisanen, T.S., Hellsten, S.K., Heikkinen, M., Nykanen, H., Jungner, H., Niskanen, A., Virtanen, M.O., Lindqvist, O.V., Nenonen, O.S., Martikainen, P.J., 2002. Fluxes of CH_4, CO_2, and N_2O in hydroelectric reservoirs Lokka and Porttipahta in the northern boreal zone in Finland. Global Biogeochem. Cy. 16(1), 1003. https://doi.org/10.1029/2000GB001316

Huttunen, J., Alm, J., Liikanen, A., Juutinen, S., Larmola, T., Hammar, T., Silvola, J., Martikainen, P., 2003. Fluxes of methane, carbon dioxide and nitrous oxide in boreal lakes and potential anthropogenic effects on the aquatic greenhouse gas emissions. Chemosphere 52, 609–621. https://doi.org/10.1016/S0045-6535(03)00243-1

Jin, B.S., 2018. Production, Distributions and Emissions of Nitrous Oxide from Reclaimed Aquaculture Ponds in the Subtropical Estuary. Fujian Normal University., doctoral dissertation, Fuzhou in Chinese.

Johnson, K.M., Hughes, J.E., Donaghay, P.L., Sieburth, J.M., 1990. Bottle-calibration static headspace method for the determination of methane dissolved in seawater. Anal. Chem. 62, 2408–2412. https://doi.org/10.1021/ac00220a030

Joyni, M.J., Kurup, B.M., Avnimelech, Y., 2011. Bioturbation as a possible means for increasing production and improving pond soil characteristics in shrimp-fish brackish water ponds. Aquaculture 318, 464–470. https://doi.org/10.1016/j.aquaculture.2011.05.019

Kosten, S., Almeida, R.M., Barbosa, I., Mendonça, R., Muzitano, I.S., Oliveira-Junior, E.S., Vroom, R.J.E., Wang, H.J., Barros, N., 2020. Better assessments of greenhouse gas emissions from global fish ponds needed to adequately evaluate aquaculture footprint. Sci. Total Environ. 748, 141247 https://doi.org/10.1016/j.scitotenv.2020.141247

Lacoste, É., Gaertner-Mazouni N., 2016. Nutrient regeneration in the water column and at the sediment-water interface in pearl oyster culture (*Pinctada margaritifera*) in a deep atoll lagoon (Ahe, French Polynesia). Estuar. Coast. Shelf. S. 182, 304–309. https://doi.org/10.1016/j.ecss.2016.01.037

Laursen, A.E., Seitzinger, S.P., 2004. Diurnal patterns of denitrification, oxygen consumption and nitrous oxide production in rivers measured at the whole-reach scale. Freshw. Biol. 49, 1448–1458. https://doi.org/10.1111/j.1365-2427.2004.01280.x

Li, S.H., Zhou, X., Cao, X.W., Chen, J.B., 2021. Insights into simultaneous anammox and denitrification system with short-term pyridine exposure: Process capability, inhibition kinetics and metabolic pathways. Front. Environ. Sci. Eng. 15. https://doi.org/10.1007/s11783-021-1433-3

Li, S.Y., Bush, R.T., Santos, I.R., Zhang, Q., Song, K.S., Mao, R., Wen, Z.D., Lu, X.X., 2018. Large greenhouse gases emissions from China's lakes and reservoirs. Water Res. 147, 13–24. https://doi.org/10.1016/j.watres.2018.09.053.

Liang, X., Xing, T., Li, J.X., Wang, B.L., Wang, F.S., He, C.Q., Hou, L.J., Li, S.L., 2019. Control of the hydraulic load on nitrous oxide emissions from cascade reservoirs. Environ. Sci. Technol. 53(20), 11745–11754. https://doi.org/10.1021/acs.est.9b03438

Lin, G.M., Lin, X.B., 2022. Bait input altered microbial community structure and increased greenhouse gases production in coastal wetland sediment. Water Res. 218, 118520. https://doi.org/10.1016/j.watres.2022.118520

Liu, S.W., Hu, Z.Q., Wu, S., Li, S.Q., Li, Z.F., Zou, J.W., 2016. Methane and nitrous oxide emissions reduced following conversion of rice paddies to inland crab-fish aquaculture in southeast China. Environ. Sci. Technol. 50 (2), 633–642. https://doi.org/10.1016/10.1021/acs.est.5b04343

Liu, X.L., Liu, C.Q., Li, S.L., Wang, F.S., Wang, B.L., Wang, Z.L., 2011a. Spatiotemporal variations of nitrous oxide (N_2O) emissions from two reservoirs in SW China. Atmos.

Environ. 45 (31), 5458–5468. https://doi.org/10.1016/j.atmosenv.2011.06.074

Liu, X.L., Li, S.L., Wang, Z.L., Han, G.L., Li, J., Wang, B.L., Wang, F.S., Bai, L., 2017. Nitrous oxide (N_2O) emissions from a mesotrophic reservoir on the Wujiang River, southwest China. Acta Geochim 36 (4), 667–679. https://doi.org/10.1007/s11631-017-0172-4

Liu, Y.S., Zhu, R.B., Ma, D.W., Xu, H., Luo, Y.H., Huang, T., Sun, L.G., 2011b. Temporal and spatial variations of nitrous oxide fluxes from the littoral zones of three alga-rich lakes in coastal Antarctica. Atmos. Environ. 45, 1464–1475. https://doi.org/10.1016/j.atmosenv.2010.12.017

Maavara, T., Lauerwald, R., Laruelle, G.G., Akbarzadeh, Z., Bouskill, N.J., Van Cappellen, P., Regnier, P., 2019. Nitrous oxide emissions from inland waters: Are IPCC estimates too high? Glob Change Biol. 25, 473–488. https://doi.org/10.1111/gcb.14504

Marescaux, A., Thieu, V., Garnier, J., 2018. Carbon dioxide, methane and nitrous oxide emissions from the human-impacted Seine watershed in France. Sci. Total Environ. 643, 247–259. https://doi.org/10.1016/j.scitotenv.2018.06.151

Massara, T.M., Malamis, S., Guisasola, A., Baeza, J.A., Noutsopoulos, C., Katsou, E., 2018. A review on nitrous oxide (N_2O) emissions during biological nutrient removal from municipal wastewater and sludge reject water. Sci. Total Environ. 596-597, 106–123. https://doi.org/10.1016/j.scitotenv.2017.03.191

Murray, R.H., Erler, D.V., Eyre, B.D., 2015. Nitrous oxide fluxes in estuarine environments: Response to global change. Global Change Biol. 21(9), 3219–3245. https://doi.org/10.1111/gcb.12923

Musenze, R.S., Grinham, A., Werner, U., Gale, D., Sturm, K., Udy, J., Yuan, Z.G., 2014. Assessing the spatial and temporal variability of diffusive methane and nitrous oxide emissions from subtropical freshwater reservoirs. Environ. Sci. Technol. 48, 14499–14507. https://doi.org/10.1021/es505324h

NOAA(National Oceanic and Atmospheric Administration), 2022. Carbon cycle greenhouse gases: Trends in N_2O. Available in: https://gml.noaa.gov/ccgg/trends_n2o/

Paudel, S.R., Choi, O., Khanal, S.K., Chandran, K., Kim, S., Lee, J.W., 2015. Effects of temperature on nitrous oxide (N_2O) emission from intensive aquaculture system. Sci. Total Environ. 518-519, 16–23. https://doi.org/10.1016/j.scitotenv.2015.02.076

Percival, J., Lindsay, P., 1997. Measurement of physical properties of sediments. In: Mudrock, A., Azcue, J. M., Mudrock, P. (Eds.), Manual of Physico-Chemical Analysis of Aquatic Sediments. CRC Press, New York, USA, pp. 7–38.

Phanwilai, S., Kangwannarakul, N., Noophan, P., Kasahara, T., Terada, A., Munakata-Marr, J., Figueroa, L.A., 2020. Nitrogen removal efficiencies and microbial communities in full-scale IFAS and MBBR municipal wastewater treatment plants at high COD:N ratio. Front. Environ. Sci. Eng. 14 (6), 115. https://doi.org/10.1007/s11783-020-1374-2

Punshon, S., Moore, R.M., 2004. Nitrous oxide production and consumption in a eutrophic coastal embayment. Mar. Chem. 91(1-4), 37-51. https://doi.org/10.1016/j.marchem.2004.04.003

Quick, A.M., Reeder, W.J., Farrell, T.B., Tonina, D., Feris, K.P., Benner, S.G., 2019. Nitrous oxide from streams and rivers: a review of primary biogeochemical pathways and environmental variables. Earth Sci. Rev. 191, 224–262. https://doi.org/10.1016/j.earscirev.2019.02.021

Rajkumar, A.N., Barnes, J., Ramesh, R., Purvaja, R., Upstill-Goddard, R.C., 2008. Methane and nitrous oxide fluxes in the polluted Adyar River and estuary, SE India. Mar. Pollut. Bull. 56 (12), 2043–2051. https://doi.org/10.1016/j.marpolbul.2008.08.005

Ravishankara, A.R., Daniel, J.S., Portmann, R.W., 2009. Nitrous oxide (N_2O): the dominant ozone-depleting substance emitted in the 21st century. Science 326, 123–125. https://doi.org/10.1126/science.1176985

Reay, D.S., Davidson, E.A., Smith, K.A., Smith, P., Melillo, J.M., Dentener, F., Crutzen, P.J., 2012. Global agriculture and nitrous oxide emissions. Nat. Clim. Change 2(6), 410-416. https://doi.org/10.1038/nclimate1458

Reisinger, A.J., Tank, J.L., Hoellein, T.J., Hall, R.O., 2016. Sediment, water column, and open-channel denitrification in rivers measured using membrane-inlet mass spectrometry. J. Geophys. Res. Biogeosci. 121(5), 1258–1274. https://doi.org/10.1002/2015JG003261

Shcherbak, I., Millar, N., Robertson, G.P., 2014. Global metaanalysis of the nonlinear response of soil nitrous oxide (N_2O) emissions to fertilizer nitrogen. PNAS, 111(25), 9199-9204. https://doi.org/10.1073/pnas.1322434111

Shrestha, N.K., Wang, J., 2018. Current and future hot-spots and hot-moments of nitrous oxide emission in a cold climate river basin. Environ. Pollut. 239, 648–660. https://doi.org/10.1016/j.envpol.2018.04.068

Stow, C.A., Walker, J.T., Cardoch, L., Spence, P., Geron, C., 2005. N_2O emissions from streams in the Neuse River Watershed, North Carolina. Environ. Sci. Technol. 39, 6999–7004. https://doi.org/10.1021/es0500355

Strokal, M., Janssen, A.B.G., Chen, X., Kroeze, C., Li, F., Ma, L., Yu, H., Zhang, F., Wang, M., 2021. Green agriculture and blue water in China: reintegrating crop and livestock production for clean water. Front. Agric. Sci. Eng. 8(1), 72-80. https://doi.org/10.15302/J-FASE-2020366

Swaney, D.P., Hong, B., Ti, C., Howarth, R.W., Humborg, C., 2012. Net anthropogenic nitrogen inputs to watersheds and riverine N export to coastal waters: a brief overview. Current Opin. Environ. Sustain. 4, 203–211. https://doi.org/10.1016/j.cosust.2012.03.004

Tan, Y.J., 2014. The Greenhouse Gases Emission and Production Mechanism from River Sediment in Shanghai. Thesis. East China Normal University, Shanghai (in Chinese).

Tian, H.Q., Xu, R.T., Canadell, J.G., Thompson, R.L., Winiwarter, W., Suntharalingam, P., Davidson, E.A., Ciais, P., Jackson, R.B., Janssens-Maenhout, G., Prather, M.J., Regnier, P., Pan, N.Q., Pan, S.F., Peters, G.P., Shi, H., Tubiello, F.N., Zaehle, S., Zhou, F., Arneth, A., Battaglia, G., Berthet, S., Bopp, L., Bouwman, A.F., Buitenhuis, E.T., Chang, J.F., Chipperfield, M.P., Dangal, S.R.S., Dlugokencky, E., Elkins, J.W., Eyre, B.D., Fu, B.J., Hall, B., Ito, A., Joos, F., Krummel, P.B., Landolfi, A., Laruelle, G.G., Lauerwald, R., Li, W., Lienert, S., Maavara, T., MacLeod, M., Millet, D.B., Olin, S., Patra, P.K., Prinn, R.G., Raymond, P.A., Ruiz, D.J., van der Werf, G.R., Vuichard, N., Wang, J.J., Weiss, R.F., Wells, K.C., Wilson, C., Yang, J., Yao, Y.Z.,

2020. A comprehensive quantification of global nitrous oxide sources and sinks. Nature 586 248–56. https://doi.org/10.1038/s41586-020-2780-0

Tian, L.L., Zhu, B., Akiyama, H., 2017. Seasonal variations in indirect N_2O emissions from an agricultural headwater ditch. Biol. Fertil. Soils 53, 651–662. https://doi.org/10.1007/s00374-017-1207-z

Tong, C., Wang, W.Q., Zeng, C.S., Marrs, R., 2010. Methane (CH4) emissions from a tidal marsh in the Min River estuary, southeast China. J. Environ. Sci. Heal. A 45, 506–516. https://doi.org/10.1080/10934520903542261

Turner, P.A., Griffis, T.J., Baker, J.M., Lee, X., Crawford, J.T., Loken, L.C., Venterea, R.T., 2016. Regional-scale controls on dissolved nitrous oxide in the Upper Mississippi River. Geophys. Res. Lett. 43, 4400–4407. https://doi.org/10.1002/2016GL068710

Venkiteswaran, J.J., Rosamond, M.S., Schiff, S.L., 2014. Nonlinear response of riverine N_2O fluxes to oxygen and temperature. Environ. Sci. Technol. 48, 1566–1573. https://doi.org/10.1021/es500069j

Wang, H.X., Zhang, L., Yao, X.L., Xue, B., Yan, W.J., 2017. Dissolved nitrous oxide and emission relating to denitrification across the Poyang Lake aquatic continuum. J. Environ. Sci. 52, 130–140. https://doi.org/10.1016/j.jes.2016.03.021

Wang, J.N., Chen, N.W., Yan, W.J., Wang, B., Yang, L.B., 2015. Effect of dissolved oxygen and nitrogen on emission of N_2O from rivers in China. Atmos. Environ. 103, 347–356. https://doi.org/10.1016/j.atmosenv.2014.12.054

Wanninkhof, R. 1992. Relationship between wind speed and gas exchange over the ocean. J. Geophys. Res. 97, 7373–7382.

Webb, J.R., Clough, T.J., Quayle, W. C., 2021. A review of indirect N_2O emission factors from artificial agricultural waters. Environ. Res. Lett. 16, 043005. https://doi.org/10.1088/1748-9326/abed00

Wrage, N., Van Groenigen, J.W., Oenema, O., Baggs, E.M., 2005. A novel dual-isotope labelling method for distinguishing between soil sources of N_2O. Rapid Commun. Mass Spectrom. 19, 3298–3306. https://doi.org/10.1002/rcm.2191

Wu, S., Zhang, T.R., Fang, X.T., Hu, Z.Q., Hu, J., Liu, S.W., Zou, J.W., 2021. Spatial-temporal variability of indirect nitrous oxide emissions and emission factors from a subtropical river draining a rice paddy watershed in China. Agr. Forest Meteorol. 307, 108519. https://doi.org/10.1016/j.agrformet.2021.108519

Wu, Y.Z., Li, Y., Wang, H.H., Wang, Z.J., Fu, X.Q., Shen, J.L., Wang, Y., Liu, X.L., Meng, L., Wu, J.S., 2021. Response of N_2O emissions to biochar amendment on a tea field soil in subtropical central China: A three-year field experiment. Agr. Ecosyst. Environ. 318, 107473. https://doi.org/10.1016/j.agee.2021.107473

Xia, X.H., Zhang, S.B., Li, S.L., Zhang, L.W., Wang, G.Q., Zhang, L., Wang, J.F., Li, Z.H., 2018. The cycle of nitrogen in river systems: Sources, transformation, and flux. Environ. Sci.-Proc. Imp. 20(6), 863–891. https://doi.org/10.1039/C8EM00042E

Xia, Y., Li, Y., Li, X., Guo, M., She, D., Yan, X., 2013. Diurnal pattern in nitrous oxide emissions from a sewage-enriched river. Chemosphere 92, 421–428. https://doi.org/10.1016/j.chemosphere.2013.01.038

Xiao, Q.T., Xu, X.F., Zhang, M., Duan, H.T., Hu, Z.H., Wang, W., Xiao, W., Lee, X.H., 2019a. Coregulation of nitrous oxide emissions by nitrogen and temperature in China's third largest freshwater lake (Lake Taihu). Limnol. Oceanogr. 64, 1070–1086. https://doi.org/10.1002/lno.11098

Xiao, Q.T., Hu, Z.H., Fu, C.S., Bian, H., Lee, X.H., Chen, S.T., Shang, D.Y., 2019b. Surface nitrous oxide concentrations and fluxes from water bodies of the agricultural watershed in Eastern China. Environ. Pollut. 251, 185–192. https://doi.org/10.1016/j.envpol.2019.04.076

Yang, H., Huang, X., Hu, J., Thompson, J. R., Flower, R. J. 2022. Achievements, challenges and global implications of China's carbon neutral pledge. Front. Environ. Sci. Eng. 16(8):111. https://doi.org/10.1007/s11783-022-1532-9

Yang, P., Lai, D.Y., Jin, B.S., Bastviken, D., Tan, L.S., Tong, C., 2017. Dynamics of dissolved nutrients in the aquaculture shrimp ponds of the Min River estuary, China: Concentrations, fluxes and environmental loads. Sci. Total Environ. 603, 256–267. http://dx.doi.org/10.1016/j.scitotenv.2017.06.074

Yang, P., Wang, D.Q., Lai, D.Y. F., Zhang, Y.F., Guo, Q.Q., Tan, L.S., Yang, H., Tong, C., Li, X.F., 2020a. Spatial variations of N_2O fluxes across the water-air Interface of mariculture ponds in a subtropical estuary in southeast China. J. Geophys. Res.-Biogeo. 125, e2019JG005605. https://doi.org/10.1029/2019JG005605

Yang, P., Yang, H., Sardans, J., Tong, C., Zhao, G.H., Peñuelas, J., Ling Li, Zhang, Y.F., Tan, L.S., Chun, K.P., Lai, D.Y.F., 2020b. Large spatial variations in diffusive CH_4 fluxes from a subtropical coastal reservoir affected by sewage discharge in southeast China. Environ. Sci. Technol. 54, 22, 14192–14203. https://doi.org/10.1021/acs.est.0c03431

Yang, P., Zhang, Y.F., Yang, H., Guo, Q.Q., Lai, D.Y.F., Zhao, G.H., Li, L., Tong, C., 2020c. Ebullition was a major pathway of methane emissions from the aquaculture ponds in southeast China. Water Res. 184, 116176. https://doi.org/10.1016/j.watres.2020.116176

Yang, P., Zhao, G.H., Tong, C., Tang, K.W., Lai, D.Y.F., Li , L., Tang, C., 2021a. Assessing nutrient budgets and environmental impacts of coastal land-based aquaculture system in southeastern China. Agr. Ecosyst. Environ. 322, 107662. https://doi.org/10.1016/j.agee.2021.107662

Yang, P., Lu, M.H., Tang, K.W., Yang, H., Lai, D.Y.F., Tong, C., Chun, K.P., Zhang, L.H., Tang, C., 2021b. Coastal reservoirs as a source of nitrous oxide: Spatio-temporal patterns and assessment strategy. Sci. Total Environ. 790, 147878. https://doi.org/10.1016/j.scitotenv.2021.147878

Yang, P., Yang, H., Lai, D.Y.F., Guo, Q.Q., Zhang, Y.F., Tong, C., Xu, C.B., Li, X.F., 2020d. Large contribution of non-aquaculture period fluxes to the annual N_2O emissions from aquaculture ponds in Southeast China. J. Hydrol. 582, 124550. doi:10.1016/j.jhydrol.2020.124550.

Ye, W.W., Sun, H., Li, Y.H., Zhang, J.X., Zhang, M.M., Gao, Z.Y., Yan, J.P., Liu, J., Wen, J.W., Yang, H., Shi, J., Zhao, S.H., Wu, M., Xu, S.Q., Xu, C.A., Zhan, L.Y., 2022. Greenhouse gas emissions from fed mollusk mariculture: A case study of a *Sinonovacula constricta* farming system. Agr. Ecosyst. Environ. 336, 108029. https://doi.org/10.1016/j.agee.2022.108029

Yin, S., Bai, J.H., Wang, W., Zhang, G.L., Jia, J., Cui, B.S., Liu, X.H., 2019. Effects of soil moisture on carbon mineralization in floodplain wetlands with different flooding frequencies. J. Hydrol. 574, 1074–1084. https://doi.org/10.1016/j.jhydrol.2019.05.007

Yogev, U., Atari, A., Gross, A., 2018. Nitrous oxide emissions from near-zero water exchange brackish recirculating aquaculture systems. Sci. Total Environ. 628-629, 603–610. https://doi.org/10.1016/j.scitotenv.2018.02.089

Yu, Z.J., Deng, H.G., Wang, D.Q., Ye, M.W., Tan, Y.J., Li, Y.J., Chen, Z.L., Xu, S.Y., 2013. Nitrous oxide emissions in the Shanghai river network: implications for the effects of urban sewage and IPCC methodology. Global Change Biol. 19, 2999–3010. https://doi.org/10.1111/gcb.12290

Yuan, J.J., Liu, D.Y., Xiang, J., He, T.H., Kang, H., Ding, W.X., 2021. Methane and nitrous oxide have separated production zones and distinct emission pathways in freshwater aquaculture ponds. Water Res. 190, 116739. https://doi.org/10.1016/j.watres.2020.116739

Yuan, J.J., Xiang, J., Liu, D.Y., Kang, H., He, T.H., Kim, S., Lin, Y.X., Freeman, C., Ding, W.X., 2019. Rapid growth in greenhouse gas emissions from the adoption of industrial-scale aquaculture. Nat. Clim. Change 9(4), 318–322. https://doi.org/10.1038/s41558-019-0425-9

Zhang, G.L., Zhang, J., Liu, S.M., Ren, J.L., Zhao, Y.C., 2010. Nitrous oxide in the Changjiang (Yangtze River) Estuary and its adjacent marine area: Riverine input, sediment release and atmospheric fluxes. Biogeosciences 7, 3505–3516. https://doi.org/10.5194/bg-7-3505-2010

Zhang, K., Tian, X.L., Dong, S.L., Feng, J., He, R.P., 2016. An experimental study on the budget of organic carbon in polyculture systems of swimming crab with white shrimp and short-necked clam. Aquaculture 451, 58–64. http://dx.doi.org/10.1016/j.aquaculture.2015.08.029

Zhang, L., Wang, L., Yin, K.D., Lü, Y., Zhang, D.R., Yang, Y.Q., Huang, X.P., 2013. Pore water nutrient characteristics and the fluxes across the sediment in the Pearl River estuary and adjacent waters, China. Estuar. Coast Shelf Sci. 133, 182–192. https://doi.org/10.1016/j.ecss.2013.08.028

Zhang, W.S., Li, H.P., Xiao, Q.T., Jiang, S.Y., Li, X.Y., 2020. Surface nitrous oxide (N_2O)

concentrations and fluxes from different rivers draining contrasting landscapes: Spatio-temporal variability, controls, and implications based on IPCC emission factor. Environ. Pollut. 263, 114457. https://doi.org/10.1016/j.envpol.2020.114457

Zhong, D.S., Wang, F., Dong, S.L., Li, L., 2015. Impact of *Litopenaeus vannamei* bioturbation on nitrogen dynamics and benthic fluxes at the sediment–water interface in pond aquaculture. Aquacult. Int. 23(4), 967–980. https://doi.org/10.1007/s10499-014-9855-6

Zhou, Y., Huang, M., Tian, H.Q., Xu, R.T., Ge, J., Yang, X.G., Liu, R.X., Sun, Y.X., Pan, S.F., Gao, Q.F., Dong, S.L., 2021. Four decades of nitrous oxide emission from Chinese aquaculture underscores the urgency and opportunity for climate change mitigation. Environ. Res. Lett. 16(11), 114038. https://doi.org/10.1088/1748-9326/ac3177

Table 1. Comparison of N_2O fluxes across the water-atmosphere interface in different aquatic ecosystems. Numbers in brackets are averages. “nd” indicates no data.

Aquatic ecosystems	Study area	N_2O flux (nmol m^{-2} h^{-1})	Reference
Aquaculture ponds	Min River Estuary, China	25.1–507.9 (216.9)	This study
	Jiulong River estuary, China	600.0–6909.1 (750.1)	Jin, 2017
	Xinghua, Jiangsu province, China	475.1–647.3 (561.6)	Fang et al., 2022
	Jurong Reservoir watershed, Eastern China	240.9–495.5 (334.1)	Xiao et al., 2019b
	Tianjin Binhai New Area, Tianjin, China	155.5–365.6 (256.6)	Hu et al., 2020
	Xinghua, Jiangsu Province, China	nd (109.2)	Liu et al., 2016
	Jiulong River Estuary, China	47.3–85.2 (66.3)	Ye et al., 2022
	Tai Lake basin, Suzhou, China	33.4–85.9 (56.5)	Yuan et al., 2021
Reservoirs / Lakes	Wenwusha Reservoir, Min River Estuary, China	-246.1–16170.5 (2590.9)	Yang et al., 2021b
	Southeast Queensland, Australia	-3.4–80.3 (9.2)	Musenze et al., 2014
	Eguzon Reservoir, France	112.5–3229.2 (716.7)	Descloux et al., 2017
	Petit Saut Reservoir, France, and Fortuna Reservoir, Panama	5625.0–9127.3 (3800.0)	Guérin et al., 2008
	Lokaa Reservoir, Finland	-79.5–259.1 (nd)	Huttunen et al., 2002
	Jurong Reservoir, Eastern China	115.9–513.6 (234.1)	Xiao et al., 2019b
	Hongjiadu Reservoir and Wujiangdu Reservoir, China	79.5–1759.1 (545.5)	Liu et al., 2011a
	Dongfeng Reservoir, China	9.1–609.1 (190.9)	Liu et al., 2017
	Lake Taihu, China	45.5–229.5 (145.5)	Xiao et al., 2019a
	Lake Mochou, Lake Tuanjie and Lake Daming, Antarctica	-809.1–1556.8 (303.0)	Liu et al., 2011b
	Poyang Lake, China	-221.1–2886.4 (nd)	Wang et al., 2017
	Lake Nakaumi, Japan	709.1–1790.9 (1070.5)	Hirota et al., 2007
	Lake Kevätön, Finland	90.0–500.1 (nd)	Huttunen et al., 2003
	China's reservoirs	nd (962.1)	Li et al., 2018
	China's reservoirs	nd (277.4)	Li et al., 2018
Rivers / Estuaries	River Avon, River Eden and River Wensum, UK	127.3–2197.7 (912.9)	Cooper et al., 2017

	River Wensum, Norfolk, UK	nd (406.8)	Hama-Aziz et al., 2017
	Chongqing metropolitan river network, China	188.6–65284.1 (10875.1)	He et al., 2017
	Xin'an Tang river, China	1470.1–3130.1 (2000.1)	Xia et al., 2013
	Shanghai river network, China	1040.1–2570.1 (nd)	Yu et al., 2013
	River Neuse, USA	-600.0–4600.1 (nd)	Stow et al., 2005
	River Millstone, USA	10.0–2140.0 (250.1)	Laursen and Seitzinger, 2004
	Adyar River, India	9.1–5100.0 (nd)	Rajkumar et al., 2008
	Sado estuary, Portugal	-90.9–156.8 (125.0)	Gonçalves et al., 2015
	Guadalete River estuary, Spain	20.5–1200.0 (470.5)	Burgos et al., 2017
	Guadalquivir Estuary, Spain	-290.9–1459.1 (354.5)	Huertas et al., 2018
	Yangtze River Estuary, China	213.6–1184.1 (554.5)	Zhang et al., 2010

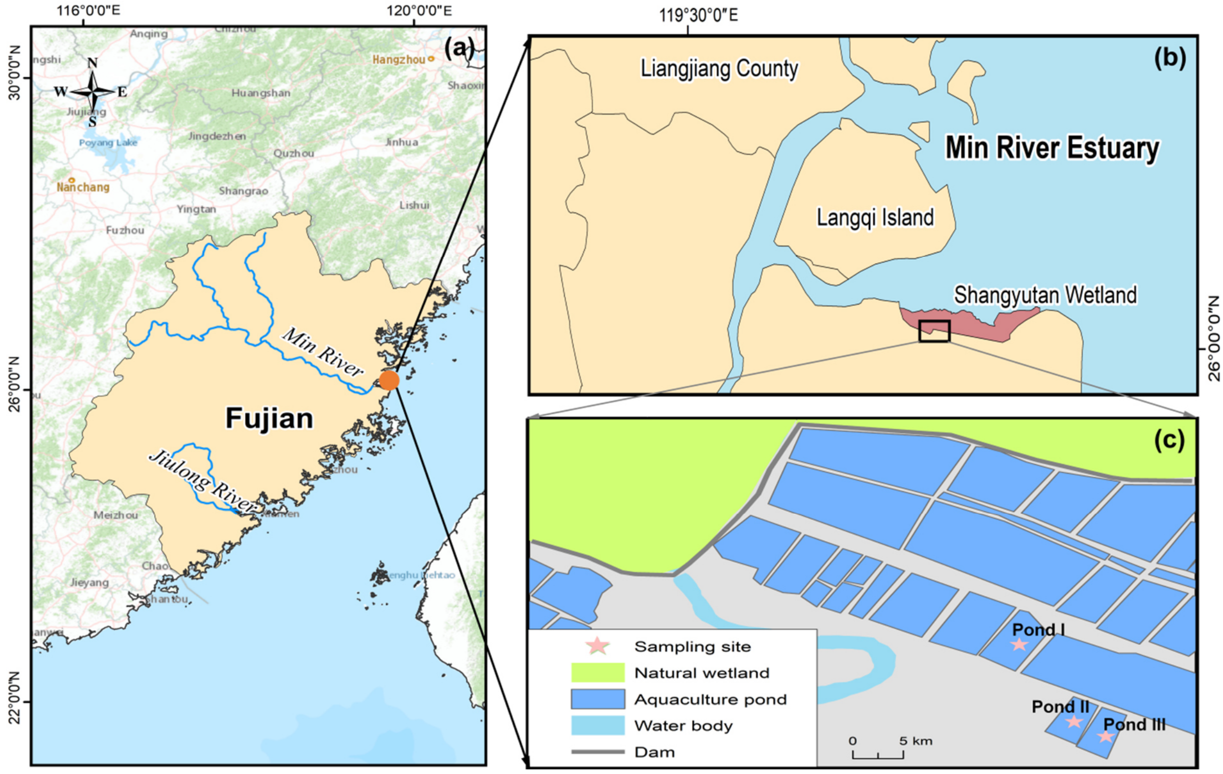

Figure 1. Map of the Shanyutan wetland within the Min River estuary showing the sampling sites in aquaculture ponds. The geographical coordinates of Pond I, Pond II and Pond III being 26°01'43"N and 119°38'30"E, 26°01'37"N and 119°38'35"E, and 26°01'36"N and 119°38'38"E, respectively.

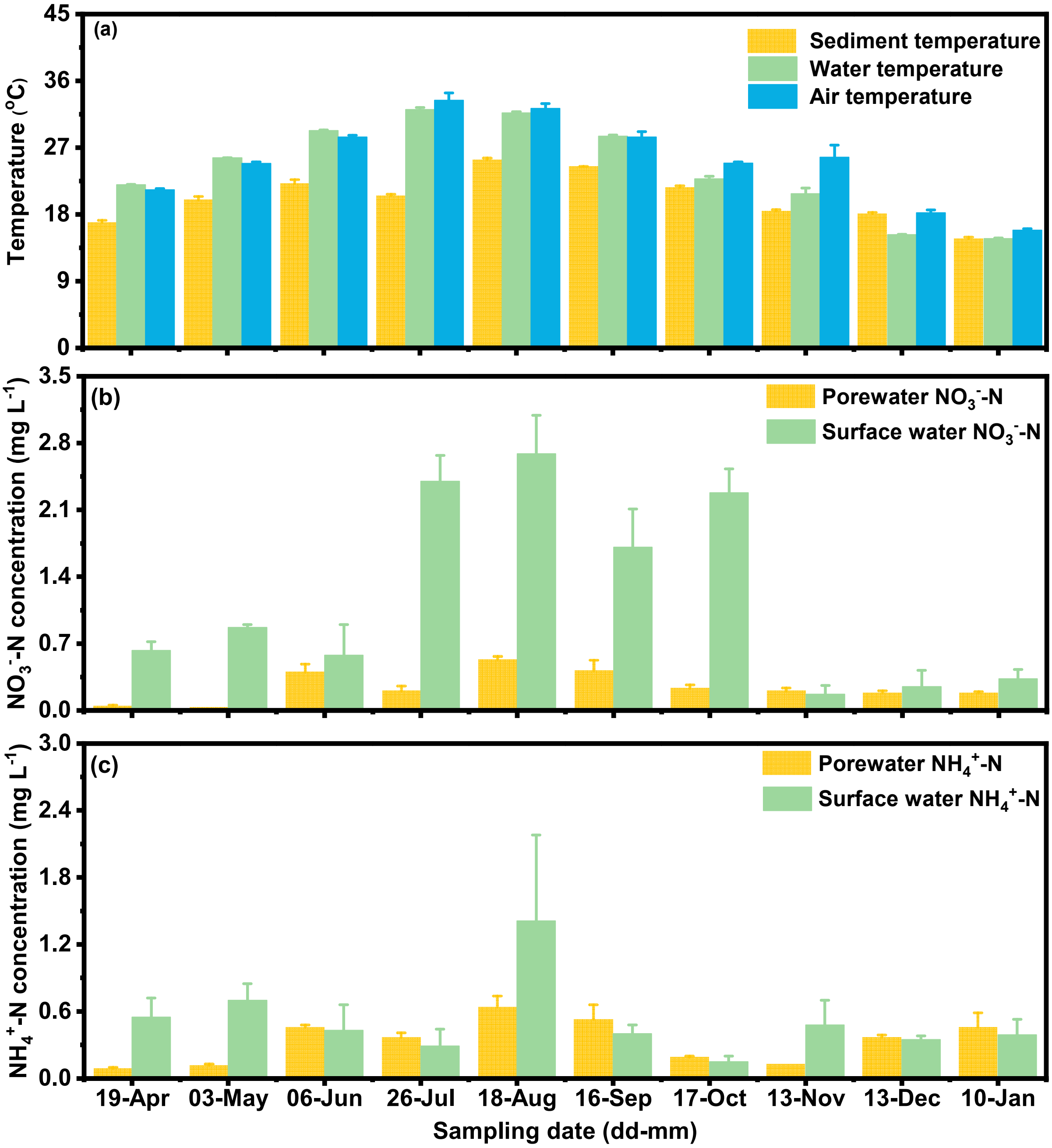

Figure 2. Monthly temperatures, NO_3^--N and NH_4^+-N concentrations in the aquaculture ponds during the farming period. The bars represent the means + 1 standard error (n = 3).

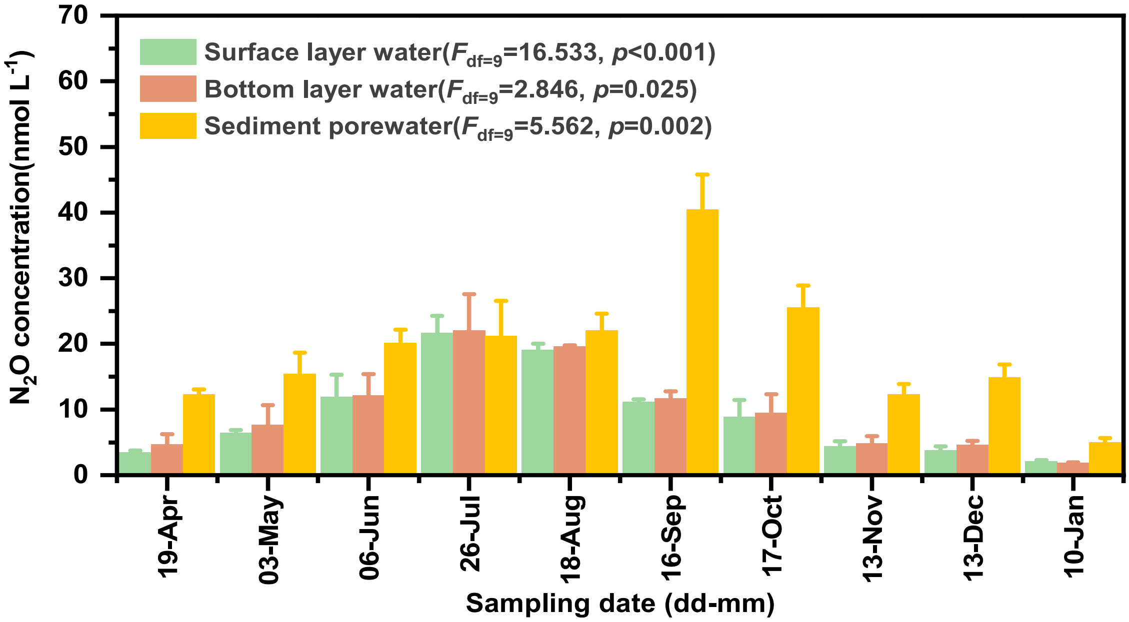

Figure 3. Monthly dissolved N_2O concentrations in the surface layer water, bottom layer water and sediment porewater of the aquaculture ponds during the farming period. The bars represent the means + 1 standard error (n = 3).

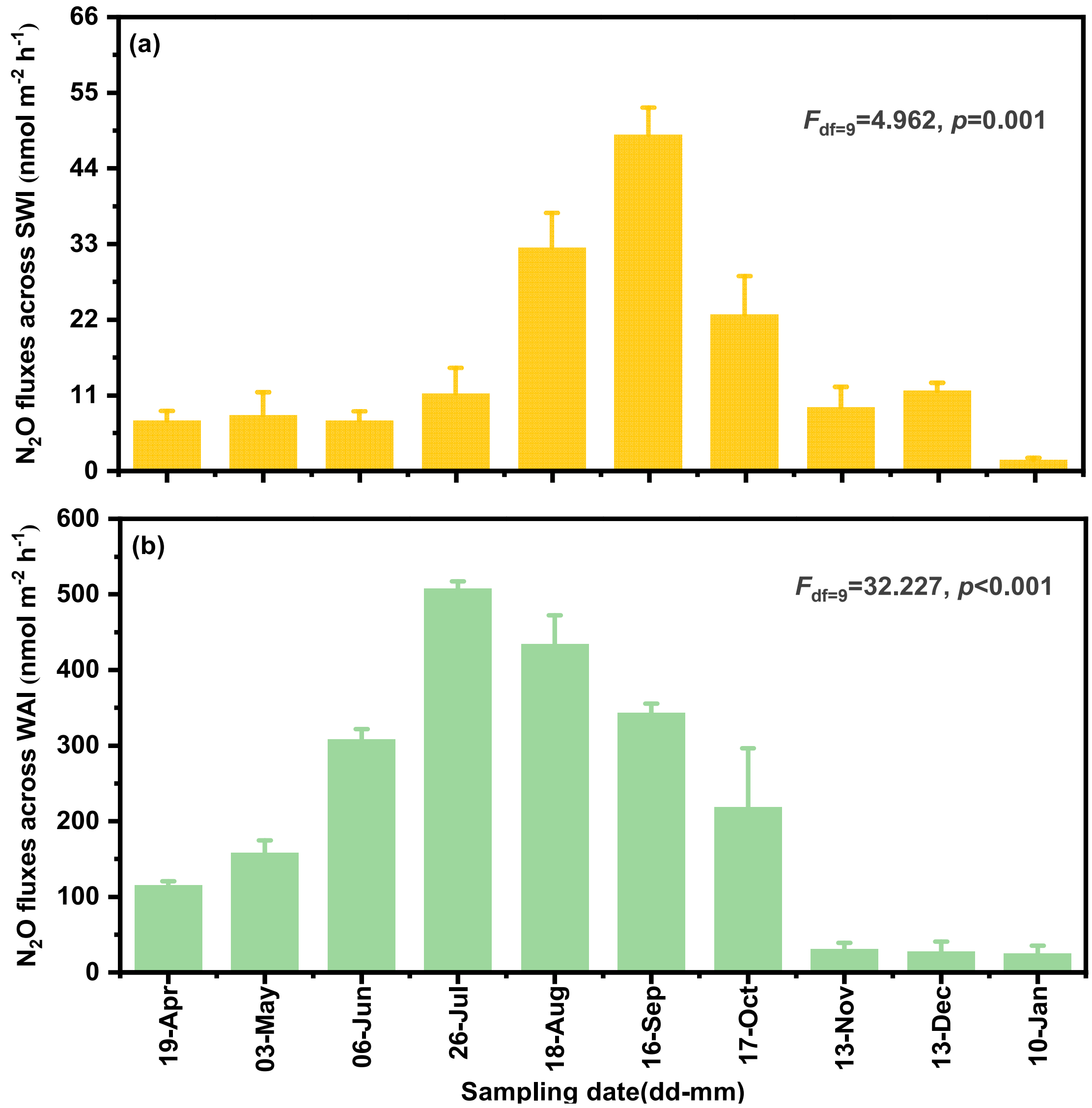

Figure 4. Monthly diffusive N_2O fluxes across (a) sediment-water interface (SWI) and (b) water-atmosphere interface (WAI) of the aquaculture ponds during the farming period. The bars represent the means + 1 standard error (n = 3).

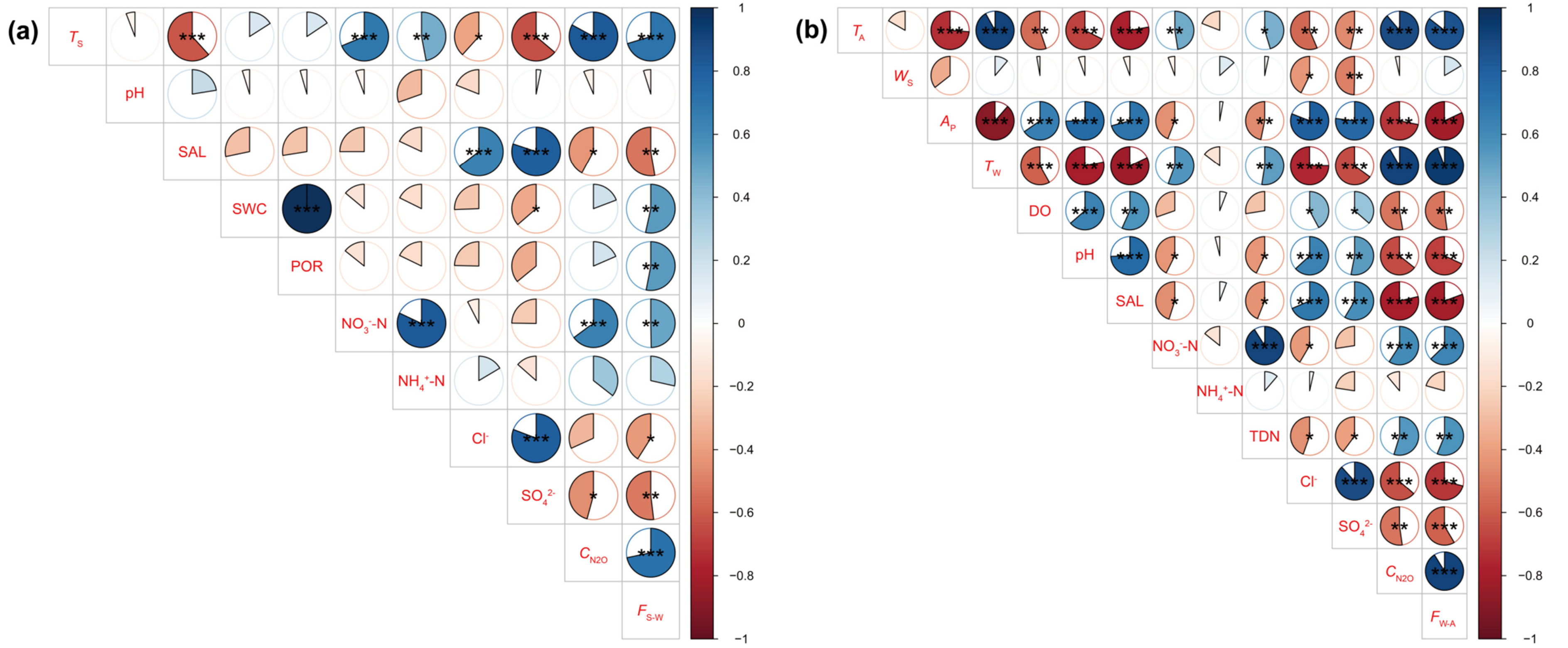

Figure 5. Correlations among environmental variables and (a) porewater N_2O concentration (C_{N2O}) and N_2O fluxes across the sediment-water interface ($F_{S\text{-}W}$), and (b) surface water N_2O concentration (C_{N2O}) and N_2O fluxes across the water-atmosphere interface ($F_{W\text{-}A}$) ($n = 30$). Color of the circle fragments indicates the direction of correlation (blue = positive; red = negative). Size of the circle fragments is proportional to the r^2 value. Asterisks indicate levels of significance ($*p < 0.05$; $**p < 0.01$; $**p < 0.001$). See main text for explanation of the abbreviations.

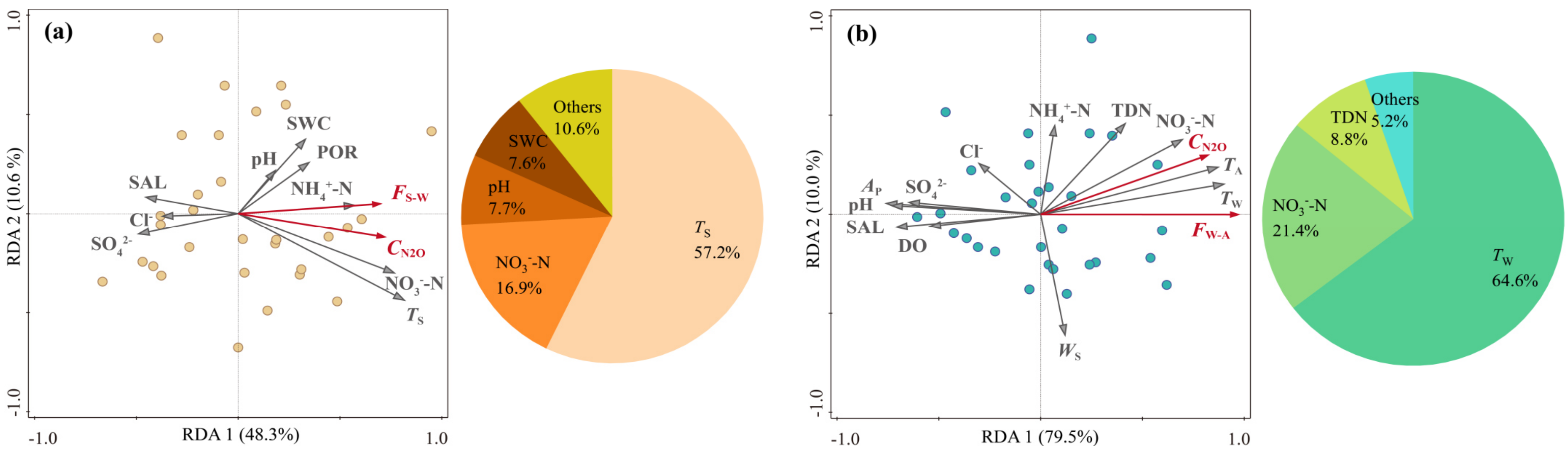

Figure 6. Results of redundancy analysis (RDA) of (a) N_2O fluxes across the sediment-water interface [or porewater N_2O concentration], and (b) N_2O fluxes across the water-atmosphere interface [or surface water N_2O concentration], showing the loadings of the different environmental variables. The pie charts show the percentages of the variance of N_2O fluxes explained by the different variables. See main text for explanation of the abbreviations.